Journal of Structural Biology **137,** 41–53 (2002)
doi:10.1006/jsbi.2002.4448

Generalized Crick Equations for Modeling Noncanonical Coiled Coils

Gerald Offer,*,[1] Matthew R. Hicks,† and Derek N. Woolfson†

*Muscle Contraction Group, Department of Physiology, Medical School, University of Bristol, University Walk, Bristol BS8 1TD, United Kingdom; and †Centre for Biomolecular Design and Drug Development, Department of Biochemistry, School of Biological Sciences, University of Sussex, Falmer BN1 9QG, United Kingdom

Received November 19, 2001, and in revised form January 23, 2002

Crick envisaged the α-helical coiled coil to result from systematic bending of an α-helix such that every seventh residue was structurally equivalent, and he derived equations for the coordinates of the backbone atoms. Crick's predictions were vindicated experimentally and coiled-coil sequences were shown to have hydrophobic residues alternately spaced 3 and 4 residues apart. Nonetheless, in some coiled coils such canonical heptad repeats are interrupted by inserts of 3 or 4 residues generating decad and hendecad motifs. The supercoiling of the coiled coils varies with the sequence pattern, being left- or right-handed in purely heptad-based or hendecad-based motifs, respectively. To model coiled coils with a mixture of motifs, we describe how Crick's equations can be modified for cases where the pitch is not constant. Using the analogy of the bending of a beam, we took the tilt angle to change linearly with distance along the major helix and the pitch of a motif to be affected by neighboring motifs depending on the rigidity of the α-helical strands. We tested our approach by fitting the two-, three-, and four-stranded noncanonical coiled coils of GrpE, hemagglutinin, and tetrabrachion. The backbone atoms of the model and crystal structures agreed with root mean square deviations of <1.1 Å.

***Key Words:* α-helical coiled coil; GrpE; hendecad; hemagglutinin; heptad; modeling; pitch; structure prediction; tetrabrachion; tilt angle.**

INTRODUCTION

Analysis of completed genome sequences suggests that as many as ~5–10% of residues in proteins are present in α-helical coiled coils (Walshaw and Woolfson, unpublished results; Mewes *et al.*, 2000; Newman *et al.*, 2000; Burkhard *et al.*, 2001), but comparatively only a few coiled-coil proteins have been structurally characterized at high resolution (Lupas, 1996; Walshaw and Woolfson, 2001). To understand better the design principles of α-helical coiled coils, there is therefore an urgent need to predict their structure from their sequence at as near the atomic level as possible.

Crick (1953a) noted that in a straight α-helix 7 residues make just under two turns. He suggested that a coiled coil could be generated by small but systematic bending of a straight α-helix so that every seventh residue was structurally equivalent. Two or more such α-helices could then pack against one another with the side chains of one strand inserting into the spaces between the side chains of the other ("knobs into holes packing"). Using this condition he derived a set of equations for defining the backbone coordinates of a coiled coil and showed that this structure accounted for the X-ray diffraction pattern of α-fibrous proteins (Crick, 1953b). He further suggested for tropomyosin that hydrophobic residues might tend to occur with alternating intervals of 3 and 4 residues (Crick, 1953a). Because the number of residues per turn in an α-helix (~3.6) is not precisely intermediate between 3 and 4, hydrophobic residues in such positions would form a left-handed stripe that winds slowly around the helix surface, that is, in the opposite sense to the winding of the α-helix itself. A coiled coil could then be formed by the hydrophobic stripes of two or more α-helices coming together and wrapping in a rope-like manner. Since Crick's suggestion, not only tropomyosin but many other coiled-coil proteins have indeed been shown to contain such a heptad repeat of hydrophobic residues (Stone *et al.*, 1975; Cohen and Parry, 1990, 1994).

High-resolution structures of proteins with a simple heptad repeat are well approximated by Crick coiled coils (O'Shea *et al.*, 1991; Phillips, 1992; Lupas, 1996; Walshaw and Woolfson, 2001). However, many coiled-coil proteins have sequences in which

[1] To whom correspondence should be addressed. Fax: +44 117 928 8923. E-mail: g.w.offer@bristol.ac.uk.

1047-8477/02 $35.00

there are occasional interruptions in the otherwise regular heptad repeat of hydrophobic residues (Brown *et al.*, 1996; Lupas, 1996; Hicks *et al.*, 1997). These occur when there is a repetition of either the interval of 4 (a "stutter") or a repetition of the interval of 3 (a "stammer") (Brown *et al.*, 1996). For example, there is a stutter in the center of the IIB region of intermediate filament proteins producing the pattern (3-4)-(3-4-**4**)-(3-4) (Parry and Fraser, 1985). In this case locally there is thus a motif containing 11 residues (a hendecad motif) rather than the canonical heptad. On the other hand, a stammer would generate the pattern (3-4)-(3-**3**-4)-(3-4) containing a 10-residue (decad) motif. In other coiled-coil proteins, heptad sequences are interrupted by an extra "skip" residue; for example, there are 4 in the skeletal myosin coiled-coil tail sequence (McLachlan and Karn, 1983; Offer, 1990). It has been proposed that such skips are best treated as two closely spaced stutters creating two adjacent hendedad motifs (Lupas *et al.*, 1995; Brown *et al.*, 1996; Hicks *et al.*, 1997).

More recently, several coiled-coil proteins have been discovered in which the hendecad or decad motifs are not just occasional insertions but recur repetitively. Examples include three proteins from *Giardia lamblia*: the median body protein with a repeating 7-10-7 (24-residue) motif, the stalked motor protein HPSR2 with a 7-11-7 (25-residue) motif, and β-giardin with a 11-7-11 (29-residue) motif (Holberton *et al.*, 1988; Marshall and Holberton, 1993, 1995; Hicks *et al.*, 1997). A shorter region displaying a repetitive 7-11-7-11-7 pattern has been observed in the nucleotide exchange factor GrpE (Harrison *et al.*, 1997), while tetrabrachion shows extensive repetition of hendecad motifs (Peters *et al.*, 1996).

Because the sequences at stutters, stammers, and skips still comprise 3- and 4-residue motifs, albeit in different combinations than the canonical 3-4 motif, the hydrophobic seam does not disappear at such interruptions but is displaced azimuthally, locally changing its tilt angle to the molecular axis (Hicks *et al.*, 1997). Consequently, the coiled coil would be expected to continue through these interruptions but with changes in geometry. A change in tilt angle would alter the local pitch of the coiled coil. Eleven residues of an α-helix make just *over* three turns. A consequence of this is that in a hendecad motif the supercoil would be expected to become *right*-handed rather than left-handed as in a heptad motif (Peters *et al.*, 1996; Hicks *et al.*, 1997). In contrast, 10 residues of an α-helix make substantially under three turns and the supercoil would be expected to be *left*-handed in a decad motif with a pitch even smaller than for a heptad (Hicks *et al.*, 1997).

In Crick's formulation, the winding of the minor helix, that is, an individual α-helical strand of the coiled coil, is taken to resemble that of a straight α-helix. An attractive feature is that only three key parameters are required to define the major helix (the supercoil): the pitch, the radius, and a parameter defining the relative rotation of the α-helical strands. The pitch is a sensitive function of the sequence even in canonical coiled coils (Phillips, 1992; Seo and Cohen, 1993; Offer and Sessions, 1995). In noncanonical coiled coils it would be expected to vary substantially, possibly even changing sign between heptad and hendecad motifs. We have therefore modified Crick's equations so that changes in pitch along the length of the coiled coil can be accommodated. Using the mechanical analogy of the bending of a beam, we have considered how the stiffness of the α-helical strands would have the effect of smoothing out abrupt changes in pitch (kinks) between motifs of different types. Our main goal was to develop a computer program based on these equations that could be used for the prediction of the three-dimensional structure of the backbone of coiled coils with noncanonical sequences. We test the applicability of this program in fitting the crystal structures of three noncanonical coiled coils. These are the double-stranded coiled coil of GrpE with alternating heptad and hendecad motifs (Harrison *et al.*, 1997), the triple-stranded $TBHA_2$ coiled coil from influenza hemagglutinin with a less regular mix of heptad and hendecad motifs (Bullough *et al.*, 1994), and the four-stranded right-handed coiled coil (RHCC) fragment from the stalk of tetrabrachion with an unusual stretch of 15 residues preceding a set of hendecad repeats (Stetefeld *et al.*, 2000).

THEORETICAL BACKGROUND

Making Noncanonical Coiled Coils with Constant Pitch

First we modified Crick's equations to create coiled coils with constant pitch for cases in which every nth residue was equivalent but where n can assume values other than 7. In Crick's formulation the coiled coil is traced out by a vector whose origin moves along the major helix rotating in a plane perpendicular to the tangent to the major helix as it does so. The rotation (measured in radians with respect to local axes) is proportional to the distance t traveled along the major helix. The constant of proportionality is called ω_1.

In passing from one atom to the equivalent atom n residues further along the coiled coil (a distance of nd along the major helix where d is the residue translation in an α-helix), this vector must rotate by an integral number of turns.

$$\omega_1 n d = 2\pi N, \qquad (1)$$

TABLE I
Values of n and N for Coiled Coils

n	N	ω_1	Pitch[a] (Å)	Tilt angle
7	2	$4\pi/7\mathbf{d}$	159	10.5°
10	3	$3\pi/5\mathbf{d}$	56	27.7°
11	3	$6\pi/11\mathbf{d}$	−398	−4.2°
15	4	$8\pi/15\mathbf{d}$	−150	−11.2°
18	5	$5\pi/9\mathbf{d}$	1144	1.5°
24	7	$7\pi/12\mathbf{d}$	94	17.5°
25	7	$14\pi/25\mathbf{d}$	423	4.0°
26	7	$7\pi/13\mathbf{d}$	−204	−8.2
29	8	$16\pi/29\mathbf{d}$	−2450	−0.7°

[a] The pitch and tilt angle are calculated for a coiled coil constructed from an α-helix with 3.617 residues per turn, an axial translation of 1.495 Å, and a major helical radius of 4.7 Å. A positive value for the pitch and tilt angle implies a left-handed supercoil; a negative value indicates a right-handed supercoil.

where N is the integer nearest to the number of turns n residues make in a straight α-helix. By supercoiling the α-helical strands, residues are enabled to occupy precisely equivalent positions every N turns of the α-helix. Table I lists the values of n that may be useful in constructing coiled-coil models. They have been chosen so that n/m lies close to an integer (N), where m is the number of residues per turn in a straight α-helix. For heptad, decad, or hendecad motifs n is 7, 10, or 11, respectively. Hence to create a noncanonical, but regularly repeating, coiled coil in which every nth residue is equivalent, we simply have to assign ω_1 the appropriate value given above.

Alternatively, if a coiled coil were to be modeled on the basis of smoothing out variations in adjacent motifs such as a repeating pattern of 7-11, 7-10-7, 7-11-7, or 11-7-11 motifs, n could be chosen as 18, 24, 25, or 29, respectively. Note that here we define motifs simply by the interval between residues in equivalent positions, not directly by the hydrophobic pattern. Hence a repeating pattern of 7-11-7 motifs is not to be regarded as precisely equivalent to a repeating 25-residue motif. In the first case the 1st, 8th, and 19th residues are in similar positions because of pitch changes, whereas in the repeating 25-residue motifs only the 1st and 26th residues are equivalent because the pitch is constant.

For a coiled coil with constant pitch, the pitch should be appropriate for n. In a straight α-helix the line connecting every nth residue is not parallel to the axis but winds around it forming the seam along which neighboring α-helical strands contact one another in the coiled coil. Fraser and MacRae (1973) deduced from this geometry the relation between the pitch, P, and m. Generalizing this relationship for noncanonical coiled coils we obtain

$$P = \pm \sqrt{\frac{d^2}{(N/n - 1/m)^2} - 4\pi^2 r_0^2}, \qquad (2)$$

where r_0 is the major helix radius. At the time of Crick's original papers the α-helix was assumed to be left-handed and, therefore, the supercoil was taken to be right-handed. Now it is known that the α-helix is right-handed and the supercoil for heptad-based coiled coils is left-handed. We shall therefore consider the supercoil to have a positive P if it is left-handed. This will occur if $N/n > 1/m$. A right-handed supercoil (negative P) will occur if $N/n < 1/m$. Table I lists the calculated pitches for $m = 3.617$ and $d = 1.495$ Å (the values for the polyalanine α-helix determined by Arnott and Dover, 1967) and with $r_0 = 4.7$ Å. No assumption need be made that the coiled coil is integral. It should be noted that the calculated pitch is left-handed for a heptad or decad motif, right-handed for a hendecad motif, and near-infinite for $n = 18$ or 29. Also note the extreme sensitivity of the pitch to changes in m.

Coiled Coils with Variable Pitch

Such equations for constant pitch are satisfactory for generating coiled coils where only one motif is present or where the aim is to construct models with supercoil smoothing over several motifs. However, in coiled coils with a mixture of motifs such as 7-11, 7-11-7, or 11-7-11, we may expect the coiled coil to show differences in local pitch between the motifs. Therefore we generalized the Crick equations for cases where the pitch is not constant but changes with distance along the coiled coil.

How does the pitch change from one motif to the next? It might have been supposed that in the center of a motif the pitch would be the same as in an infinite stretch of that motif but would change toward its neighboring motifs. If that were the case, in a coiled coil where heptads alternated with hendecads, the pitch would abruptly shift from left-handed to right-handed, producing a zigzag structure. However, this would require the α-helical strands to bend very sharply. For example, if the tilt angle in the center of a heptad motif were 10.5° and that in the center of an adjoining hendecad motif were −4.2°, this would require the α-helical strands to bend by 14.7° over a stretch of at most nine residues or ~13.5 Å. That would require a radius of curvature as low as 53 Å. If the bending were to occur only over say the "e", "f", and "g" residues of the heptad motif, the radius of curvature would be only 18 Å. In globular proteins the radius of curvature of α-helices is around 60 Å and in canonical coiled coils it is as high as 150 Å (Blundell *et al.*, 1983; Barlow and Thornton, 1988). It is pertinent that in the crystal structure of GrpE where heptads alternate with hendec-

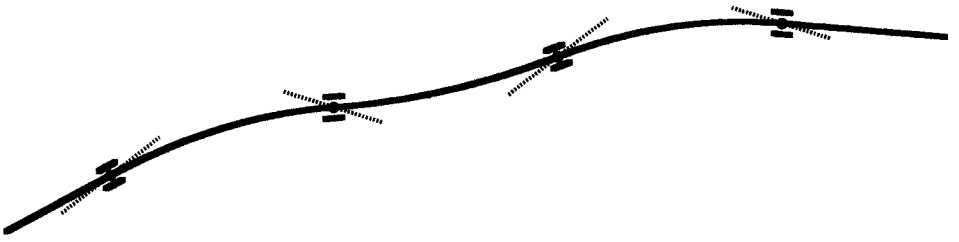

FIG. 1. Diagram of a beam bent at four sites by the application of couples. The beam is represented by the long thick wavy line, and each of the four sleeves, by which a couple is applied, is represented by a pair of short thick lines. The unstrained direction of each of the sleeves is shown by a dotted line.

ads the α-helical strands are nearly straight and lie side by side (Harrison *et al.*, 1997). Yet in coiled coils where there are stretches of uninterrupted hendecad or uninterrupted heptad sequences the supercoiling is markedly right-handed or left-handed, respectively. This strongly suggests that neighboring motifs interact in such a way as to smooth out differences. We suggest that in regions where heptads are adjacent to hendecads the very different tilt angles required for these two motifs for optimal interaction in the core of the coiled coil cannot simultaneously be satisfied because of the rigidity of the α-helical strands. The result is a compromise between the two tilt angles. However, in a stretch of a single type of motif repeat no such compromise needs to be reached and the tilt angle can readily adopt the optimum value for that type of motif. In other words the pitch of a motif is not an absolute but depends on the nature of the neighboring motifs.

Therefore we need to model the mechanical effect which one motif has on its neighboring motifs. We were not concerned with attempting a detailed modeling of the myriad atomic interactions that underlie such an interaction, but instead with adopting a more pragmatic approach likening each α-helical strand to a beam. We supposed that each motif, if unstrained, adopts the tilt angle appropriate for an infinite stretch of that motif but due to the stiffness of the strands actually adopts some other tilt angle closer to that of its neighbors.

Consider first the curvature induced by applying couples of equal and opposite magnitude C to the ends of an initially straight rod of circular cross-sectional radius a and length l. In the standard method for analyzing the bending of a cantilevered beam (see, for example, Gere, 2001), the internal bending moment generated by the tension of fibrous elements on the outside of the curvature and by the compression of fibrous elements on the inside of the curvature is equated with the external bending moment. Applying couples to both ends of the beam, rather than clamping the beam at one end and applying a load at the other, produces a simpler result: the beam is deformed into a circular arc of radius R given by

$$C = \frac{\pi Y a^4}{4R}, \tag{3}$$

where Y is the Young's modulus of the beam.

If the angle to a fixed line made by a tangent to the beam at any point distance s from one end is θ, $1/R$ may be replaced by $d\theta/ds$.

We suppose in this mechanical analogy that the couples are generated by inserting the ends of the beam into sleeves that are spring-loaded. Unstrained, the sleeves adopt angles θ_1 and θ_2 to the fixed line but when strained by inserting the beam into them they adopt angles $\theta_1 + \delta\theta_1$ and $\theta_2 + \delta\theta_2$. If the spring constant is K, the couples applied to the two ends of the beam are $K\delta\theta_1$ and $K\delta\theta_2$ so that

$$\begin{aligned} K\delta\theta_1 = -K\delta\theta_2 &= \frac{\pi Y a^4}{4}\frac{d\theta}{ds} \\ &= \frac{\pi Y a^4\,(\theta_2 + \delta\theta_2 - \theta_1 - \delta\theta_1)}{4l}, \end{aligned} \tag{4}$$

Note that if Y is large, (i.e., the beam is stiff) or K is small (i.e., the springs are weak), the angles adopted by the sleeves, $(\theta_1 + \delta\theta_1)$ and $(\theta_2 + \delta\theta_2)$, are identical and equal to $(\theta_1 + \theta_2)/2$ so the beam is straight. If, however, Y is small or K is large, $\delta\theta_1$ and $\delta\theta_2$ are small and the sleeves adopt the unstrained angles θ_1 and θ_2. If $K = (\pi Y a^4)/(2l)$, then $\delta\theta_1 = (\theta_2 - \theta_1)/4$ and so the angles adopted are $((3\theta_1/4) + \theta_2/4)$ and $(\theta_1/4 + (3\theta_2/4))$. Hence values of $(\pi Y a^4/2lK)$ around 1 provide a convenient marker of this intermediate situation.

We now have to extend this treatment to the case where the beam is inserted into many (n) spring-loaded sleeves along its length so that the couples generated are $K\delta\theta_1$, $K\delta\theta_2$, $K\delta\theta_3$, . . . $K\delta\theta_n$. The bending of a beam into a wave in this manner is illustrated in Fig. 1 for the case in which there are four sleeves. Note that for the general case

$$\sum_{i=1}^{i=n} \delta\theta_i = 0. \tag{5}$$

It is supposed that the unstrained angles θ_1, θ_2, . . . θ_n of these sleeves differ but the spring constants K are identical.

Consider a segment of the beam between the mth and the $(m + 1)$th sleeve. The first m couples and the last $(n - m)$ couples contribute in equal and opposite directions to the straining of this segment into a circular arc. Hence

$$K\sum_{i=1}^{i=m}\delta\theta_i = \frac{\pi Y a^4}{4s_m}(\theta_{m+1} + \delta\theta_{m+1} - \theta_m - \delta\theta_m), \quad (6)$$

where s_m is the contour length of this segment.

Or writing $(4K/\pi Ya^4)$ as a single constant b,

$$bs_m\sum_{i=1}^{i=m}\delta\theta_i = (\theta_{m+1} + \delta\theta_{m+1} - \theta_m - \delta\theta_m). \quad (7)$$

There are n-1 of these equations so, together with Eq. (5), the values of all $\delta\theta_i$ and hence all the actual angles $(\theta_i + \delta\theta_i)$ of the beam at the sleeves are determined. In each segment the value of θ depends linearly on s (although the constant of proportionality, and hence radii of the arcs, differs between segments) so the entire shape of the beam is known. Note that the value of b governs the shape of the beam. If b is low, the beam is nearly straight; if b is high, the beam is very wavy. Consequently we shall refer to b as the smoothing parameter.

We shall use this example of a beam twisted by a series of spring-loaded sleeves into a wave as an analogy in constructing a coiled coil with variable pitch. But it should be noted that whereas the beam is bent into a wave in two dimensions, the coiled coil is bent in three dimensions. Each of the sleeves corresponds to the center of a motif that in an infinite stretch of these identical motifs would adopt the unstrained tilt angle α_i but instead, due to the finite rigidity of the α-helical strands, adopts a different perturbed tilt angle $(\alpha_i + \delta\alpha_i)$. The tilt angle is thus analogous to the angle, θ, the beam makes to a fixed direction, while the distance, t, measured along the major helix is analogous to the distance, s, measured along the length of the beam. Using this analogy, the tilt angle α at any point along the major helix is taken to change linearly between the center of one motif and the center of a neighboring motif. A consequence of making this analogy is that the sum of the tilt angles at the centers of the motifs throughout the length of the coiled coil is invariant as the smoothing parameter b is altered.

The local pitch P at any point on the major helix may then be determined from α:

$$P = \frac{2\pi r_0}{\tan\alpha}. \quad (8)$$

Note that if b were very small (i.e., if the strands were very stiff or the interactions a motif makes to adopt the "ideal" tilt angle for that motif very weak), the tilt angles of all the motifs would become identical and the pitch would be constant throughout the coiled coil. If, however, b were very large (i.e., if the strands were very compliant or the constraints on a motif to adopt the "ideal" tilt angle very strong), all $\delta\alpha_i$ would be zero and in the center of each motif the strands would adopt a tilt angle appropriate for an infinite stretch of that motif. Hence by adjusting a single parameter, b, the effects of altering the compliance of the strands can be explored. A convenient marker for an intermediate situation occurs when $b = 2/t_m$ or ~0.15 for a segment between heptad and hendecad motifs, where t_m is the length measured along the major helix between the centers of the mth and $(m + 1)$th motifs. Note that a motif not only affects its immediate neighbors but also has a small influence on more remote motifs. Figure 2 shows a plot of the tilt angle against the distance along the major helix for a pattern of 7-11-7-11-7-11-7-11 motifs with a range of b values. With $b = 10$, the tilt angles at the centers of the heptad or hendecad motifs are similar to those obtained for repeating polymers of purely heptad or purely hendecad motifs (10.5° and −4.2°, respectively). As b decreases, the differences between these tilt angles decrease and at $b = 0.01$ only small fluctuations in tilt angle are seen between motifs.

The Major Helix

We had to define the axial and azimuthal coordinates of any point along the major helix a distance t from its origin. In Crick's case of constant pitch, the translation ΔZ along the molecular axis in traversing a length Δt of the major helix is given by

$$\Delta Z = \frac{|P|\Delta t}{\sqrt{P^2 + 4\pi^2 r_0^2}} = \cos\alpha\,\Delta t. \quad (9)$$

In our case where P varies with t, this had to be replaced by

$$\Delta Z = \int\frac{|P|dt}{\sqrt{P^2 + 4\pi^2 r_0^2}} = \int\cos\alpha\,dt. \quad (10)$$

If the tilt angle α is a linear function of t and has the value α_1 at t_1 and α_2 at t_2, then this may be integrated to give

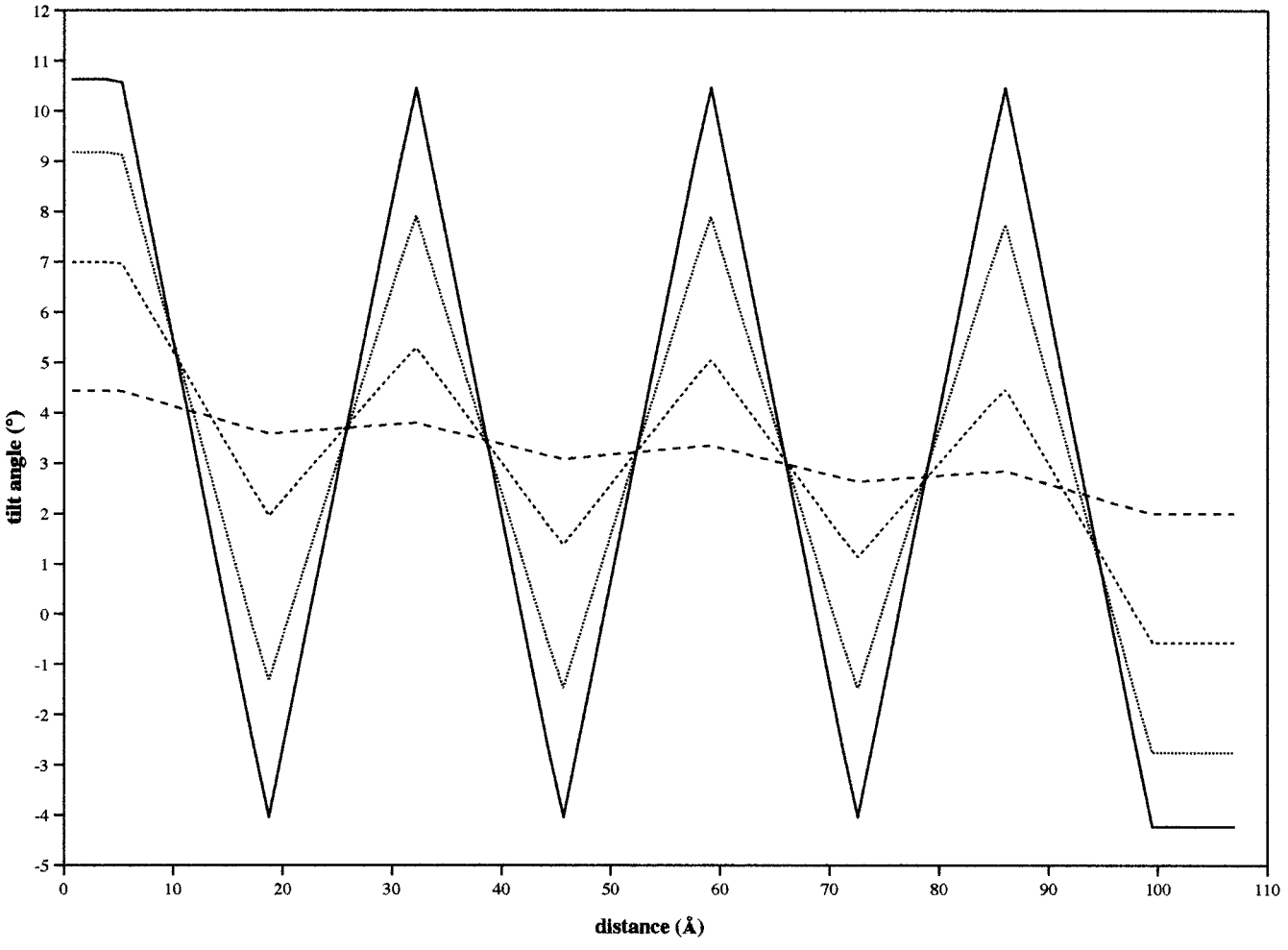

FIG. 2. Effect of changing the smoothing parameter b on the variation of tilt angle along an idealized noncanonical coiled coil with a 7-11-7-11-7-11-7-11 pattern of motifs. – – – $b = 0.01$; - - - $b = 0.1$; · · · $b = 0.5$; — $b = 10$.

$$\Delta Z = \frac{t_2 - t_1}{\alpha_2 - \alpha_1} (\sin \alpha_2 - \sin \alpha_1). \qquad (11)$$

In Crick's case of constant pitch, the azimuthal rotation $\Delta\psi$ around the molecular axis in traversing a length Δt of the major helix is given by

$$\Delta\psi = \pm \frac{2\pi\Delta t}{\sqrt{P^2 + 4\pi^2 r_0^2}} = \sin \alpha \frac{\Delta t}{r_0}. \qquad (12)$$

The azimuthal rotation is taken to be positive for a left-handed supercoil (positive P) and negative for a right-handed supercoil (negative P).

If P varies with t, this must be replaced with

$$\Delta\psi = \pm 2\pi \int \frac{dt}{\sqrt{P^2 + 4\pi^2 r_0^2}} = \frac{1}{r_0} \int \sin \alpha \, dt. \qquad (13)$$

Again an explicit solution is possible if α is a linear function of t:

$$\Delta\psi = \frac{t_2 - t_1}{r_0 (\alpha_2 - \alpha_1)} (\cos \alpha_1 - \cos \alpha_2). \qquad (14)$$

By applying Eqs. (11) and (14) separately to each segment and summing them, the cylindrical coordinates (Z, ψ) of any point a distance t along the major helix can be calculated.

The Minor Helix

Having defined the major helix, it was necessary to determine how rapidly the coiled coil should be traced out by the rotating vector. Since the value of ω_1 differs for different motifs, we supposed that ω_1 too would vary along the length of a coiled coil containing mixed motifs. We assigned ω_1 throughout each heptad, decad, or hendecad motif a value iden-

tical to that for an infinite polymer of that motif. But other options, such as allowing ω_1 to depend on the local tilt angle, are also possible.

The Backbone Coordinates

With the above considerations, it was possible to calculate the coordinates of the atoms of the backbone of the coiled coil with variable pitch. To derive such coordinates, Crick used local axes whose origin followed the path of the major helix, the local z' axis being tangential to the major helix and the local x' axis always pointing directly away from the molecular axis. He derived equations for the transformation from this local frame to the global frame. Suppose the origin of the local axes is on the major helix with cylindrical coordinates (Z, ψ) and hence Cartesian coordinates ($r_0 \cos \psi$, $-r_0 \sin \psi$, Z). Any point x' y' z' referred to the local axes has coordinates in the global frame given by

$$x = r_0 \cos \psi + x' \cos \psi + y' \cos \alpha \sin \psi - z' \sin \alpha \sin \psi \quad (15)$$

$$y = -r_0 \sin \psi - x' \sin \psi + y' \cos \alpha \cos \psi - z' \sin \alpha \cos \psi \quad (16)$$

$$z = Z + y' \sin \alpha + z' \cos \alpha. \quad (17)$$

The coiled coil is generated by a vector whose origin moves along the major helix rotating in a right-handed manner by ω_1 radians per unit of t traveled. For the Crick case of constant pitch, ω_1 is constant and the local coordinates of any point on a continuous coiled coil are

$$x' = r_1 \cos(\omega_1 t + \varphi_1) \quad (18)$$

$$y' = r_1 \sin(\omega_1 t + \varphi_1) \quad (19)$$

$$z' = 0, \quad (20)$$

where r_1 is the radius of the minor helix and φ_1 is the phase angle, both of which depend on the type of atom.

For the case of noncanonical coiled coils where ω_1 is itself a function of t, Eq. (18) and (19) must be replaced with

$$x' = r_1 \cos(\int \omega_1 dt + \varphi_1) \quad (21)$$

$$y' = r_1 \sin(\int \omega_1 dt + \varphi_1). \quad (22)$$

Combining Eqs. (15), (16), (17), (21), and (22) we arrive at the Cartesian coordinates of a point on the continuous coiled coil

$$x = r_0 \cos \psi + r_1 \cos(\int \omega_1 dt + \varphi_1) \cos \psi + r_1 \sin(\int \omega_1 dt + \varphi_1) \cos \alpha \sin \psi \quad (23)$$

$$y = -r_0 \sin \psi - r_1 \cos(\int \omega_1 dt + \varphi_1) \sin \psi + r_1 \sin(\int \omega_1 dt + \varphi_1) \cos \alpha \cos \psi \quad (24)$$

$$z = Z + r_1 \sin(\int \omega_1 dt + \varphi_1) \sin \alpha. \quad (25)$$

For an atom of a particular type in residue i of the coiled coil, the translation t and phase angle φ_1 in the above equations are given by

$$t = z_{\text{rel}} + (i - 1)\, d \quad (26)$$

$$\varphi_1 = \varphi_1^{\text{ref}} + \varphi_{\text{rel}} - \omega_1 z_{\text{rel}} + \frac{z_{\text{rel}} \sin \alpha}{r_0}, \quad (27)$$

where z_{rel} and φ_{rel} are the axial and azimuthal polar coordinates of that type of atom relative to a reference atom (conveniently C_α or C_β) in a straight α-helix and φ_1^{ref} is the value of φ_1 for that reference atom. φ_1^{ref} therefore serves as a convenient measure of the relative rotation of the α-helical strands. (φ_1^{ref} would be termed φ_1^α if the reference atom is the C_α atom and φ_1^β if it were the C_β atom.) The value of φ_1^{ref} is assumed to be identical in a mixture of heptad, decad, and hendecad motifs.

METHODS

We wrote a program BEAMMOTIFCC.c to incorporate the above principles. BEAMMOTIFCC calculates the backbone coordinates for any mixture of motifs, not necessarily a regularly repeating pattern. The input variables include the following: m and d, the residues per turn and axial translation per residue of a straight α-helix; r_0, the major helical radius; φ_1^β, the relative rotation of the α-helical strands; and b, the smoothing parameter determined by both the compliance of the α-helical strands and the strength of the interface. The number of α-helical strands can be altered, rotational symmetry about the molecular axis being assumed. The unstrained tilt angles of the major helix at the centers of different motifs (e.g., at the centers of heptad and hendecad motifs) were calculated from m, d, and r_0. The starting values for the m and d parameters for the straight α-helix were

TABLE II
Parameters for Model Coiled Coils to Best Fit Native Coiled Coils

Protein	Pattern of motifs	Number of strands	Residues superposed[a]	rms (Å)	m	d (Å)	r_0 (Å)	φ_1^β	b	Tilt angles at centers of motifs
Noncanonical coiled coils										
GrpE[b]	7-11-7-11-7	2	44–86 (2)	1.08	3.589	1.490	4.84	214.6	0.007	2.5° 1.9° 2.2° 1.9° 2.5°
$TBHA_2$ of hemagglutinin	11-7-11-7-7-7-11-11	3	40–105 (3)	0.96	3.629	1.500	6.84	214.8	0.025	3.8° 6.7° 6.2° 9.3° 9.8° 8.3° 3.5° 1.1°
RHCC of tetrabrachion	8-7-11-11-11	4	4–51 (4)	0.84	3.661	1.489	7.45	207.2	0.063	−20.4° −2.0° −1.3° −0.9° −0.8°
Canonical coiled coils										
GCN4	7-7-7-7	2	2–29 (2)	0.30	3.628	1.506	4.86	217.7	—	
GCN4 p-II	7-7-7-7	3	2–29 (3)	0.39	3.608	1.530	6.65	216.1	—	
GCN4 p-LI	7-7-7-7	4	2–29 (4)	0.66	3.593	1.520	7.56	219.5	—	
Cortexillin	7-7-7-7-7-7-7-7-7-7-7-7-7	2	243–343 (2)	0.94	3.636	1.501	4.91	211.7	—	
Tropomyosin	7-7	2	36–50 (2)	0.30	3.580	1.518	4.99	212.2	—	
			22–36 (1)	0.14	3.619	1.514	4.27	210.3	—	

[a] The number in parentheses is the number of chains of the coiled coil used in the superposition.
[b] In the refinement of GrpE the axial stagger of the two chains was allowed to alter. In the refined model this stagger was 1.7 Å.

taken from the values for polyalanine (Arnott and Dover, 1967). The starting value of r_0 was taken to be 4.7 Å for a double-stranded coiled coil (Offer and Sessions, 1995), 6.7 Å for a triple-stranded coiled coil (Harbury *et al.*, 1994), and 7.6 Å for a four-stranded coiled coil (Harbury *et al.*, 1993). The starting value of φ_β^1 was taken to be 210° (Offer and Sessions, 1995).

The output is a pdb file of the coordinates of the backbone atoms. Coiled-coil structures were viewed in the molecular graphics application InsightII (MSI, San Diego, CA). The root mean square (rms) deviation of the heavy atoms of the backbone over the corresponding atoms in the crystal structure was determined after the superposition of the model and experimental structures. The idealized structures were refined by varying m, d, r_0, φ_1^β, and b to minimize the rms deviation by the downhill simplex method (Nelder and Mead, 1965) modified to run from a shell script (Offer *et al.*, 2000).

BEAMMOTIFCC is not limited by the length of the coiled coil. It can satisfactorily deal with a hendecad in the center of 20 heptads maintaining the correct phase delay across the stutter regardless of the degree of smoothing. However, it should not be used where there are long repeats (>10) of the same type of motif, due to errors incurred using Eq. (7) in calculating the set of $\delta\alpha_i$ when the first is near zero. Such a situation would be best handled by making a separate calculation for the region where the pitch is expected to be essentially constant (using a program based on the unmodified Crick equations) and combining the result with a calculation made with BEAMMOTIFCC for the region over which the pitch is expected to change.

RESULTS

At present there are only a few examples of noncanonical coiled motifs in the Brookhaven database (Hicks *et al.*, 2002). These are either based on heptad–hendecad sequence combinations or are purely hendecad-based. For our purpose, namely, testing the modeling capabilities of BEAMMOTIFCC, we selected three structures to cover the range of different coiled-coil oligomer states from two- to four-stranded; at present there is only one example of a five-stranded coiled-coil structure, namely, COMP (Malashkevich *et al.*, 1996), and this is based on canonical heptad repeats. All the structures we discuss are parallel coiled coils. The results of modeling these noncanonical coiled coils are shown in Table II, where they are compared with the modeling of canonical coiled coils, including two-stranded coiled coils of GCN4 (O'Shea *et al.*, 1991), tropomyosin (Brown *et al.*, 2001), and cortexellin (Burkhard *et al.*, 2000), of three-stranded GCN4 p-II (Harbury *et al.*, 1994), and of four-stranded GCN4 p-LI (Harbury *et al.*, 1993).

GrpE (1dkg)

First we modeled the two-stranded coiled coil of the nucleotide exchange factor GrpE from *Escherichia coli*. The crystal structure of this factor has been determined when bound to the ATPase domain of the heat shock protein DnaK (Harrison *et al.*, 1997). The GrpE structure is an asymmetric dimer with the interface formed from two long parallel helices that form a rather distorted homodimeric coiled coil. The sequence in this region shows heptads interspersed with hendecads to form a 7-11-7-11-7 pattern. Since 18 residues in an α-helix make almost exactly five turns, this sequence pattern would be expected to straighten the coiled coil and produce two helical strands that lie side by side; indeed the crystal structure strikingly confirms the almost complete absence of supercoiling. We modeled residues 44–86 with alternating heptads and hendecad motifs in the pattern 7-11-7-11-7. Because in GrpE the two strands in the coiled coil are axially staggered we allowed the chains of the model to

stagger during refinement. Using the starting parameters the rms deviation when the backbone heavy atoms of residues 44 to 86 of the GrpE model were superposed over the crystal structure was 1.38 Å and this improved to 1.08 Å on refinement. By viewing the α-helical strands in the crystal structure one behind the other (Fig. 3), the slight left-handed supercoiling in the N-terminal half of the structure is seen, while in the C-terminal half the two α-helical strands are essentially straight. The model reproduces this feature satisfactorily. During refinement the *b* value fell to a low level and correspondingly the tilt angles showed only small differences between the centers of the heptad and hendecad motifs (Table II).

Hemagglutinin (1htm)

Next, we modeled the three-stranded coiled coil from the integral membrane glycoprotein hemagglutinin of influenza virus. A large domain forming the host–receptor binding site is situated at one end of the coiled-coil stem. At the other end of this stem is the domain that anchors the protein into the viral membrane. Prior to fusion, residues 76–126 of the HA_2 chains form a relatively short triple-stranded coiled-coil stem, and, despite their high coiled-coil potential (Carr and Kim, 1993), residues 38–55 and 56–75 form a separate short α-helix and extended strand, respectively, which pack against the outside of the coiled coil (Wilson *et al.*, 1981). However, when the pH is lowered to 5, the chains refold extensively (Carr and Kim, 1993; Bullough *et al.*, 1994). The short α-helix and extended strand become incorporated into the coiled coil at its N-terminal end; conversely the C-terminal end of the coiled coil refolds to form a loop and separate α-helix. This large conformational change is thought to cause the relocation of the fusion peptide 100 Å toward the target membrane. The crystal structure of $TBHA_2$, the proteolytic product of hemagglutinin after exposure to the pH of membrane fusion (Bullough *et al.*, 1994), shows residues 40 to 105 of each HA_2 chain forming a continuous three-stranded coiled coil. The coiled coil commences with a slightly left-handed supercoil with a long pitch, followed by a more pronounced left-handed helix with a shorter pitch and then a region that is almost straight. We modeled residues 40–105 as a pattern of 11-7-11-7-7-7-11-11 motifs with Ser 40 as the *g* residue of the first heptad as suggested by Bullough *et al.* (1994). With the starting parameters the rms deviation was 1.2 Å but on refinement this improved to 0.96 Å. The model has somewhat too high a pitch and major helical radius at the C-terminal end of the coiled coil but otherwise the broad features of the supercoiling are well demonstrated by the model, with the N- and C-terminal ends of the coiled coil being very underwound and the central region exhibiting a clear left-handed supercoiling (Fig. 4).

Tetrabrachion (1fe6)

Finally, we modeled the RHCC fragment of the exceptionally stable four-stranded coiled coil of the stalk of the glycoprotein tetrabrachion from the thermophilic archaebacterium *Staphylothermus marinus* (Peters *et al.*, 1996). In this coiled coil, a predominantly heptad repeat of hydrophobic residues shifts to a predominantly hendecad repeat after a proline residue. The crystal structure of RHCC, a 52-residue fragment in the C-terminal segment of the stalk, confirmed earlier predictions (Peters *et al.*, 1996) that in this predominantly hendecad region the coiled coil should be right-handed (Stetefeld *et al.*, 2000). In the original phasing of the sequence (Peters *et al.*, 1996), this fragment was considered to consist exclusively of hendecad repeats. However, in the crystal structure the first 18 residues have a more pronounced right-handed supercoiling than the remainder of the coiled coil and the phasing of the sequence in this region was therefore reassessed. It was concluded that residues 12–15 should be treated as an additional stutter (Stetefeld *et al.*, 2000); this reassignment allows more hydrophobic residues in the "a" and "h" positions of the hendecad. There is therefore a stretch of 15 residues from 4 to 18 before the hendecad repeats start that Stetefeld *et al.* considered to consist of an octad plus a heptad. We therefore modeled residues 4–18 in this way and residues 19–52 as a set of hendecad repeats. With the starting parameters, the rms deviation when the backbone heavy atoms of residues 4–51 of all four chains were superposed on the crystal structure was 2.3 Å. On refinement this rms deviation improved considerably to 0.84 Å. The fit to the crystal structure is shown in Fig. 5. The change from pronounced right-handed supercoiling in residues 4–18 to a weaker right-handed supercoiling in residues 19–52 is well modeled.

DISCUSSION

In this paper we describe the generalization of the Crick equations for modeling coiled-coil structures to deal with the variable pitch exhibited by noncanonical sequences, that is, where the heptad repeat is interrupted or replaced by decad or hendecad motifs. Our software can cope with any combination of motifs and is not restricted to simple, regularly repeating patterns. The advantage of the equations is that only five intuitively straightforward parameters need to be specified to define a noncanonical coiled coil, regardless of the pattern of the motifs. These are *m*, the residues per turn, and *d*, the axial translation per residue of a straight α-helix, r_0, the

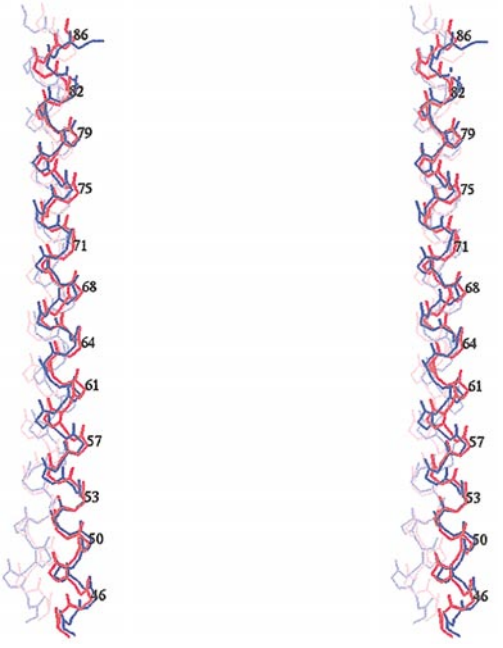

FIG. 3. Stereoview of the superposition of the refined model (red) and the crystal structure (blue) of GrpE (PDB entry 1dkg). Only the backbone atoms of residues 44 to 86 of the coiled coil are displayed. The model assumed a pattern of 7-11-7-11-7 motifs. The coiled coils are viewed in such a direction that the two α-helical strands cross one another and the rear strand has been shown in paler colors. The N-terminal end is at the bottom and residue numbers at intervals of 3 or 4 residues are indicated.

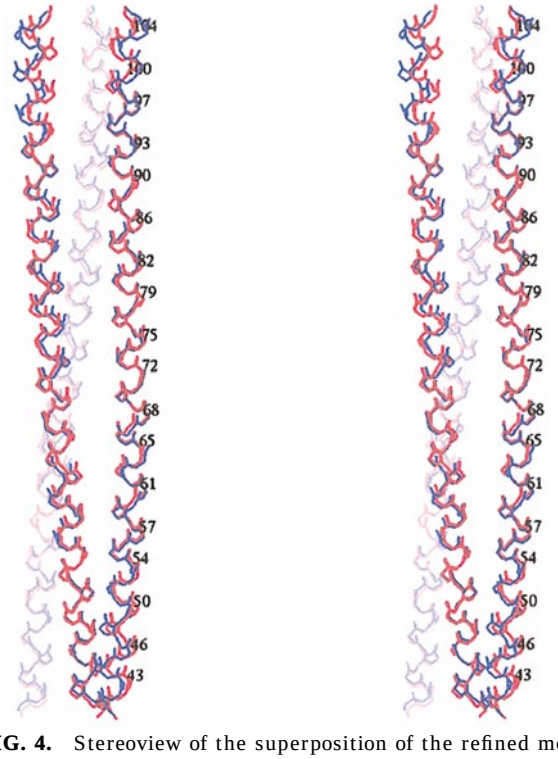

FIG. 4. Stereoview of the superposition of the refined model (red) and the crystal structure (blue) of $TBHA_2$ from influenza hemagglutinin (PDB entry 1htm). Only the backbone atoms of residues 40 to 105 are displayed. The model assumed a pattern of 11-7-11-7-7-7-11-11 motifs. The N-terminal end is at the bottom and residue numbers at intervals of 3 or 4 residues are indicated.

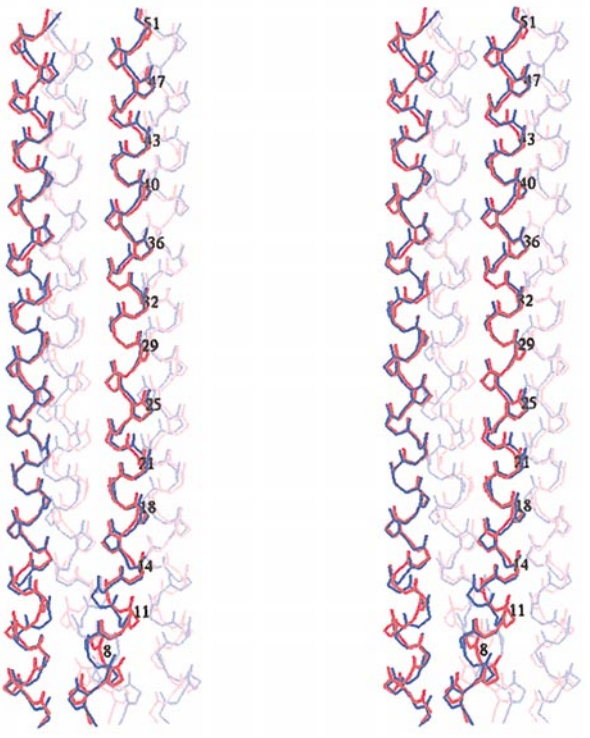

FIG. 5. Stereoview of the superposition of the refined model (red) and the crystal structure (blue) of the RHCC from tetrabrachion (PDB entry, 1fe6). Only the backbone atoms of residues 4 to 51 are displayed. The model assumed an 8-7-11-11-11 pattern of motifs. The two α-helical strands at the rear are shown in paler colors to allow the front two strands to be seen more clearly. The N-terminal end is at the bottom and residue numbers at intervals of 3 or 4 residues are indicated.

major helix radius, φ_1^β, the parameter defining the relative rotation of the α-helical strands, and b, the smoothing parameter that is determined by the compliance of the α-helical strands and the strength of the interface. This is a remarkably small number considering the complexity of the coiled coil exhibited for example by hemagglutinin. Note that the pitches of the motifs making a pattern (e.g., heptads and hendecads) are not allowed to vary independently; they are related to each other through m and d in Eq. (2). It is fortunate that the five parameters are known within quite close limits. Table II shows that in our refined models, excluding the rather special case of tropomyosin segments, d varies between only 1.489 and 1.530 Å and m between 3.584 and 3.661. Even allowing for the marked sensitivity of pitch to m, this puts considerable constraints on the modeling. If information about pitch is available (e.g., for the myosin coiled-coil tail the pitch of the heptad region is known to lie close to 145 Å), this places even further constraints. r_0, the radius of the supercoil, increases as the number of strands increases and values within an accuracy of about 0.2 Å are available for two, three, and four strands (O'Shea *et al.*, 1991; Harbury *et al.*, 1993, 1994). φ_1^β

TABLE III
Suggested Parameters for Modeling Coiled Coils of Unknown Structure

Number of strands	m	d (Å)	r_0 (Å)	φ_1^β	b
2	3.63	1.49	4.9	212°	0.03
3	3.63	1.49	6.8	212°	0.03
4	3.63	1.49	7.5	212°	0.03

is known by modeling for two-stranded coiled coils (Offer and Sessions, 1995) and confirmed here in modeling of GCN4. φ_1^β assumes similar values (207°–219°) for the refined two-, three-, and four-stranded noncanonical and canonical coiled-coil models (Table II). In all three of our refined models of the noncanonical coiled coils the value of b was low, well below the benchmark intermediate value of 0.15, indicating a considerable degree of smoothing of the tilt angles. Nevertheless even with the lowest value of b obtained with the GrpE model, a residual variation of the tilt angles from heptad to hendecad is apparent. The parameters we suggest might be used as a starting point for modeling two-, three-, and four-stranded coiled coils are summarized in Table III.

This approach should allow us to calculate a plausible model of the backbone of a coiled coil for which the crystal structure is not available. The likely error in the position of the atoms is probably less than 1.5 Å. This is of similar magnitude to the difference observed in crystal structures between biochemically identical strands in multistranded coiled coils (Harbury *et al.*, 1993). In Crick's concept, bending to produce the supercoil causes the atoms on the outside of the coiled coil to move further apart and those in the interior to move together. This results in systematic perturbations to the bond lengths, bond angles, and torsion angles for the residues within a motif. However, as shown by the rms deviations for fitting short canonical coiled coils, for example, GCN4, such effects are smaller than 0.3 Å. To create the predicted model, it is of course first necessary to establish the number of strands, either by physical chemical measurements or by deducing this from the sequence features (Berger *et al.*, 1995; Woolfson and Alber, 1995; Wolf *et al.*, 1997). It is obviously also crucial to analyze the sequence looking, for example, for hydrophobic residues to define the phasing and hence the pattern of motifs (Brown *et al.*, 1996; Hicks *et al.*, 1997). In many cases this is straightforward but the example of the RHCC fragment of tetrabrachion indicates that in some cases the phasing may be apparent only after the crystal structure has been obtained (Brown *et al.*, 1996; Stetefeld *et al.*, 2000).

The idealized models generated by these equations can be considered to be in effect a "smoothed" version of the real coiled coil in which the effect of side-chain packing in the inner and outer cores of the interface results in residue-by-residue small fluctuations in pitch (Philips, 1992; Seo and Cohen, 1993; Offer and Sessions, 1995). Such idealized models may nevertheless be directly useful, for example, in predicting the winding of the supercoil and thereby explaining the appearance of electron micrographs of the molecules or predicting the interactions which such coiled coils make in higher-order assemblies. For example, the equations could be used to model the long α-helical coiled-coil tails of the skeletal and smooth myosin molecules having, respectively, four or three skip residues. This would allow us to see if the underwinding of the two α-helical strands at each skip had similar or different orientations along the length of the tail. It would also enable us to extend to three dimensions McLachlan and Karn's (1983) analysis of the charge–charge interaction between neighboring coiled-coil tails in the thick filament backbone.

If the goal was to predict the structure of a coiled coil at the atomic level, the side chains, in conformations appropriate to the azimuthal position within the motif, would need to be added and the models refined by energy minimization or molecular dynamics. Starts have been made in predicting the side-chain conformations in the interface (Nilges and Brunger, 1993; Harbury *et al.*, 1994; Offer and Sessions, 1995), and the complex intrahelical and interhelical interactions, but this remains a goal for the future. We have shown, however, that the backbone of coiled-coil proteins that have been crystallized are well represented by a generalization of the Crick equations, which, therefore, afford a convenient starting point in prediction.

It was noticeable that on refinement of our models of noncanonical coiled coils the value of b fell to a low value. This implies that natural coiled coils do not tolerate sharp changes in pitch along their lengths. Rather, changes in pitch at the boundaries between putative heptad and hendecad motifs are blurred and smoothed out locally. This is well seen in the crystal structure of GrpE where heptads alternate with hendecads; the pitch does not abruptly shift from left-handed to right-handed in a zigzag manner but appears to be nearly constant. Nevertheless the examples of RHCC and hemagglutinin clearly show that the pitch in a coiled coil can change substantially over a longer distance. It would be interesting to design a coiled coil where a run of heptad motifs was followed by a run of hendecad motifs, first to show that strong left-handed supercoiling can coexist with strong right-handed supercoiling and second to gauge how rapidly the pitch changes at the

boundary. We suggest that the behavior of natural coiled coils is due to the relative stiffness of the α-helical strands allowing the tilt angle to change only slowly over a distance. All this raises the question of whether the heptads and hendecads in a mixed sequence are able to make the same kind of interactions in the core of a coiled coil as they can in a purely heptad-based or hendecad-based sequence. For example, it was of interest to know whether the "a" and "d" layers of the heptads of GrpE are similar to those of canonical coiled coils and thus whether the dimer interface can be considered to be that of a true coiled coil. This would enable us to decide whether it is meaningful to consider GrpE as consisting of alternating heptad and hendecad motifs or whether it is more properly treated as having 18-residue motifs. Using the recommended default cutoff values, our program SOCKET (Walshaw and Woolfson, 2001) did not identify any clear knobs into holes interactions consistent with a two-stranded coiled coil. However, when the parameters were slightly relaxed to allow more distant knobs into holes, interaction layers of knob residues were identified. These layers had faults consistent with the out-of-register helix–helix interactions. Thus the helical interface of GrpE can be considered a rather loose and distorted noncanonical coiled coil. Clearly more work is required to determine whether these features and the near-constant pitch found in GrpE are the general case for alternating heptad and hendecad motifs or whether coiled coils exist (or can be designed) where the pitch changes more abruptly (forming a zigzagging structure) because both types of motif form strong interfaces with well-defined knobs into holes packing.

REFERENCES

Arnott, S., and Dover, S. D. (1967) Refinement of bond angles of an α-helix. *J. Mol. Biol.* **30,** 209–212.

Barlow, D. J., and Thornton, J. M. (1988) Helix geometry in proteins. *J. Mol. Biol.* **201,** 601–619.

Berger, B., Wilson, D. B., Wolf, E., Tonchev, T., Milla, M., and Kim, P. S. (1995) Predicting coiled coils by use of pairwise residue correlations. *Proc. Natl. Acad. Sci. USA* **92,** 8259–8263.

Blundell, T., Barlow, D., Borkakoti, N., and Thornton, J. (1983) Solvent-induced distortions and the curvature of α-helices. *Nature* **306,** 281–283.

Brown, J. H., Cohen, C., and Parry, D. A. D. (1996) Heptad breaks in α-helical coiled coils: Stutters and stammers. *Proteins* **26,** 134–145.

Brown, J. H., Kim, K.-H., Jun, G., Greenfield, N., Dominguez, R., Volkmann, N., Hitchcock-DeGregori, S. E., and Cohen, C. (2001) Deciphering the design of the tropomyosin molecule. *Proc. Nat. Acad. Sci. USA* **98,** 8496–8501.

Bullough, P. A., Hughson, F. M., Skehel, J. J., and Wiley, D. C. (1994) Structure of influenza hemagglutinin at the pH of membrane fusion. *Nature* **371,** 37–43.

Burkhard, P., Kammerer, R. A., Steinmetz, M. O., Bourenkov, G. P., and Aebi, U. (2000) The coiled coil trigger site of the rod domain of cortexillin I unveils a distinct network of interhelical and intrahelical salt-bridges. *Struct. Fold. Des.* **8,** 223–230.

Burkhard, P., Stetefeld, J., and Strelkov, S. V. (2001) Coiled coils: A highly versatile protein folding motif. *Trends Cell Biol.* **11,** 82–88.

Carr, C. M., and Kim, P. S. (1993) A spring-loaded mechanism for the conformational change of influenza hemagglutinin. *Cell* **73,** 823–832.

Cohen, C., and Parry, D. A. D. (1990) α-Helical coiled coils and bundles: How to design an α-helical protein. *Proteins* **7,** 1–15.

Cohen, C., and Parry, D. A. D. (1994) α-Helical coiled coils: More facts and better predictions. *Science* **263,** 488–489.

Crick, F. (1953a) The packing of α-helices: Simple coiled-coils. *Acta Crystallogr.* **6,** 689–697.

Crick, F. (1953b) The Fourier transform of a coiled-coil. *Acta Crystallogr.* **6,** 685–689.

Fraser, R. D. B., and MacRae, T. P. (1973) Conformation in Fibrous Proteins and Related Synthetic Polypeptides. Academic Press, London.

Gere, J. M. (2001) Mechanics of Materials, 5th ed., Brooks/Cole, Pacific Grove, CA.

Harbury, P. B., Khang, T., Kim, P. S., and Alber, T. (1993) A switch between two-, three-, and four-stranded coiled coils in GCN4 leucine zipper mutants. *Science* **262,** 1401–1407.

Harbury, P. B., Kim, P. S., and Alber, T. (1994) Crystal structure of an isoleucine-zipper trimer. *Nature* **371,** 80–83.

Harrison, C. J., Hayer-Hartl, M., Di Liberto, M., Hartl, F.-U., and Kuriyan, J. (1997) Crystal structure of the nucleotide exchange factor GrpE bound to the ATPase domain of the molecular chaperone DnaK. *Science* **276,** 431–435.

Hicks, M. R., Holberton, D. V., Kowalczyk, C., and Woolfson, D. N. (1997) Coiled-coil assembly by peptides with non-heptad sequence motifs. *Folding Design* **2,** 149–158.

Hicks, M. R., Walshaw, J., and Woolfson, D. N. (2002) Investigating the tolerance of coiled-coil peptides to nonheptad sequence inserts. *J. Struct. Biol.* **137,** 73–81.

Holberton, D., Baker, D. A., and Marshall, J. (1988) Segmented α-helical coiled-coil structure of the protein giardin from the *Giardia* cytoskeleton. *J. Mol. Biol.* **204,** 789–795.

Lupas, A. (1996) Coiled-coils: New structures and new functions. *Trends Biochem. Sci.* **21,** 375–382.

Lupas, A., Müller, S., Goldie, K., Engel, A. M., Engel, A., and Baumeister, W. (1995) Model structure of the Ompα rod, a parallel four-stranded coiled coil from the hyperthermophilic eubacterium *Thermotoga maritima*. *J. Mol. Biol.* **248,** 180–189.

Malashkevich, V. N., Kammerer, R. A., Efimov, V. P., Schulthess, T., and Englel, J. (1996) The crystal structure of a five-stranded coiled coil in COMP: A prototype ion channel? *Science* **274,** 761–765.

Marshall, J., and Holberton, D. V. (1993) Sequence and structure of a new coiled-coil protein from a microtubule bundle in *Giardia*. *J. Mol. Biol.* **231,** 521–530.

Marshall, J., and Holberton, D. V. (1995) *Giardia* gene predicts a 183 kDa nucleotide-binding head-stalk protein. *J. Cell Sci.* **108,** 2683–2692.

McLachlan, A., and Karn, J. (1983) Periodic features in the amino acid sequence of nematode myosin rod. *J. Mol. Biol.* **164,** 605–626.

Mewes, H. W., Frishman, D., Gruber, C., Geier, B., Haase, D., Kaps, A., Lemcke, K., Mannhaupt, G., Pfeiffer, F., Schuller, C., Stocker S., and Weil, B. (2000) MIPS: A database for genomes and protein sequences. *Nucleic Acids Res.* **28,** 37–40.

Nelder, J. A., and Mead, R. (1965) The simplex method for function minimisation. *Comput. J.* **7,** 308–313.

Newman, J. R. S., Wolf, E., and Kim, P. S. (2000) A computationally directed screen identifying interacting coiled coils from *Saccharomyces cerevisiae*. *Proc. Natl. Acad. Sci. USA* **97,** 13203–13208.

Nilges, M., and Brunger, A. T. (1993) Successful prediction of the coiled coil geometry of the GCN4 leucine zipper domain by simulated annealing: Comparison to the X-ray structure. *Proteins* **15,** 133–146.

Offer, G. (1990) Skip residues correlate with bends in the myosin tail. *J. Mol. Biol.* **216,** 213–218.

Offer, G., and Sessions, R. (1995) Computer modelling of the α-helical coiled coil: Packing of side chains in the inner core. *J. Mol. Biol.* **249,** 967–987.

Offer, G., Knight, P. J., Burgess, S. A., Alamo, L., and Pádrón, R. (2000) A new model for the surface arrangement of myosin molecules in tarantula thick filaments. *J. Mol. Biol.* **298,** 239–260.

O'Shea, E. K., Klemm, J. D., Kim, P. S., and Alber, T. (1991) X-ray structure of the GCN4 leucine zipper, a two-stranded, parallel coiled coil. *Science* **254,** 539–544.

Parry, D. A. D., and Fraser, R. D. B (1985) Intermediate filament structure. 1. Analysis of IF protein sequence data. *Int. J. Biol. Macromol.* **7,** 203–213.

Peters, J., Baumeister, W., and Lupas, A. (1996) Hyperthermostable surface layer protein tetrabrachion from the archaebacterium *Staphylothermus marinus*: Evidence for the presence of a right-handed coiled coil derived from the primary structure. *J. Mol. Biol.* **257,** 1031–1041.

Phillips, G. N. (1992) What is the pitch of the α-helical coiled coil? *Proteins* **14,** 425–429.

Seo, J., and Cohen, C. (1993) Pitch diversity in α-helical coiled coils. *Proteins* **15,** 223–234.

Stetefeld, J., Jenny, M., Schulthess, T., Landwehr, R., Engel, J., and Kammerer, R. A. (2000) Crystal structure of a naturally occurring parallel right-handed coiled coil tetramer. *Nat. Struct. Biol.* **7,** 772–776.

Stone, D., Sodek, J., Johnson, P., and Smillie, L. B. (1975) In Proceedings of the 9th FEBS Meeting, Vol. 31, pp. 125–136, Akademiai Kiado, Budapest, and North Holland, Amsterdam.

Walshaw, J., and Woolfson, D. N. (2001) SOCKET: A program for identifying and analysing coiled-coil motifs within protein structures. *J. Mol. Biol.* **307,** 1427–1450.

Wilson, I. A., Skehel, J. J., and Wiley, D. C. (1981) Structure of the hemagglutinin membrane glycoprotein of influenza virus at 3 Å. *Nature* **289,** 366–373.

Wolf, E., Kim, P. S., and Berger, B. (1997) MultiCoil: A program for predicting two and three stranded coiled coils. *Protein Sci.* **6,** 1179–1189.

Woolfson, D. N., and Alber, T. (1995) Predicting oligomerization states of coiled coils. *Protein Sci.* **4,** 1596–1607.